Compound ES of Cytochrome *c* Peroxidase Contains a Trp π-Cation Radical: Characterization by CW and Pulsed Q-Band ENDOR Spectroscopy

Jennifer E. Huyett,† Peter E. Doan,† Ryszard Gurbiel,† Andrew L. P. Houseman,† Mohanram Sivaraja,† David B. Goodin,*,‡ and Brian M. Hoffman*,†

Contribution from the Department of Chemistry, Northwestern University, 2145 Sheridan Road, Evanston, Illinois 60208, and Department of Molecular Biology, MB8, The Scripps Research Institute, 10666 North Torrey Pines Road, La Jolla, California 92037

Received March 28, 1995®

Abstract: The fully oxidized state of cytochrome *c* peroxidase (CcP), called ES, contains two oxidizing equivalents, one as an oxyferryl heme and the other as an organic radical on an amino acid residue. The unusual electron paramagnetic resonance spectrum of ES has been shown to be due to a weak, distributed exchange coupling between the two paramagnetic redox centers (Houseman, A. L. P.; Doan, P. E.; Goodin, D. B.; Hoffman, B. M. *Biochemistry* **1993**, *32*, 4430−4443). Various residues have been proposed as the radical site over the years. In this paper, continuous wave and pulsed Q-band electron nuclear double resonance (ENDOR) spectroscopy on samples isotopically enriched with [^{13}C]-, [^{15}N]-, and [^{2}H]tryptophan confirm that the radical is located on Trp-191, as previously proposed. The data show that an exchangeable proton with $A(^1H) \approx 16$ MHz is associated with N1H of the Trp π-cation radical and not with C2H that has been labilized in the radical state. In addition, through a combination of ^{13}C and ^{2}H labeling we have determined the hyperfine couplings at $g = 2.01$ for $^{13}C\beta$, and the $C\beta H_2$, N1H, and C2H protons. An analysis of these couplings based on the magnetic properties of the spin-coupled heme-radical redox cluster of ES has yielded spin densities for the radical in agreement with those predicted for the cation radical, confirming the assignment and suggesting that the radical is not greatly perturbed by N1H···O hydrogen bonding to the carboxylate of Asp-235. This paper, thus, completes the characterization of the active site of compound ES as being comprised of an oxyferryl heme coupled to the Trp-191 π-cation radical by a weak spin exchange.

Introduction

Yeast cytochrome *c* peroxidase (CcP) catalyzes the H_2O_2-dependent oxidation of ferrocytochrome *c*.[1,2]

$$CcP + H_2O_2 \rightarrow ES + H_2O$$

$$ES + 2\text{Cyt } c(Fe^{II}) + 2H^+ \rightarrow CcP + 2\text{Cyt } c(Fe^{III}) + H_2O$$

Like other heme peroxidases such as horseradish peroxidase (HRP) and catalase, the resting-state ferriheme of CcP becomes oxidized by two equivalents during the reaction with peroxide,[1−4] forming a stable intermediate. This fully oxidized state is called compound ES in the case of CcP and compound I in the case of HRP and catalase.[4] In all cases, one of the equivalents is stored as the $S = 1$ oxyferryl (Fe(IV)) moiety and the other equivalent is stored as an organic radical. For compound I the site of the latter is the porphyrin,[4] but it has long been known that for compound ES the second equivalent resides on an amino acid residue.[5,6] Thus, CcP is the first in an emerging class of enzymes that use an amino acid as a radical site in their mechanism of function.[7,8]

Over the years several sites have been proposed as the location of the radical in compound ES.[1,9] An obvious choice was tyrosine or tryptophan, and the crystal structure of the enzyme (Figure 1) shows that Trp-51 is only ~3.6 Å above and parallel to the porphyrin ring, leading to the suggestion that it is a likely site of oxidation.[10,11] However, the electron paramagnetic resonance (EPR) envelope is anomalously broad for an aromatic π-radical, extending from fields below $g = 2.04$ to fields well above the maximum intensity at $g = 2.01$ (Figure 2). Such properties first led to the suggestion of a peroxy radical[5] and later to that of a nucleophilically stabilized methionyl radical.[12]

The cloning and expression of CcP led to renewed efforts to identify the radical using site-directed mutants. The Met-172 → Ser and Trp-51 → Phe mutants gave unperturbed EPR signals upon oxidation; thus, neither Trp-51 nor Met-172 is the radical

* To whom correspondence should be addressed.
† Northwestern University.
‡ The Scripps Research Institute.
® Abstract published in *Advance ACS Abstracts*, August 15, 1995.

(1) Yonetani, T. *J. Biol. Chem.* **1965**, *240*, 4509−4514.
(2) Coulson, A. F. W.; Erman, J. E.; Yonetani, T. *J. Biol. Chem.* **1971**, *246*, 917−924.
(3) Yonetani, T. In *The Enzymes*; Boyer, P. D., Ed.; Academic Press: Orlando, FL, 1976; Vol. 13, pp 345−361.
(4) Dawson, J. H. *Science* **1988**, *240*, 433−439.
(5) Wittenberg, B. A.; Kampa, L.; Wittenberg, J. B.; Blumberg, W. E.; Peisach, J. *J. Biol. Chem.* **1968**, *243*, 1863−1870.
(6) Hoffman, B. M.; Roberts, J. E.; Brown, T. G.; Kang, C. H.; Margoliash, E. *Proc. Natl. Acad. Sci. U.S.A.* **1979**, *76*, 6132−6136.
(7) Volker-Wagner, A. F.; Frey, M.; Neugebauer, F. A.; Schäfer, W.; Knappe, J. *Proc. Natl. Acad. Sci. U.S.A.* **1992**, *89*, 996−1000.
(8) Essenmacher, C.; Kim, Sang-T.; Atamian, M.; Babcock, G. T.; Sancar, A. *J. Am. Chem. Soc.* **1993**, *115*, 1602−1603.
(9) Yonetani, T.; Schleyer, H.; Ehrenberg, A. *J. Am. Chem. Soc.* **1966**, *241*, 3240−3243.
(10) Finzel, B. C.; Poulos, T. L.; Kraut, J. *J. Biol. Chem.* **1984**, *259*, 13027−13036.
(11) Poulos, T. L.; Finzel, B. C. *Pept. Protein Rev.* **1984**, *4*, 115−171.
(12) Hoffman, B. M.; Roberts, J. E.; Kang, C. H.; Margoliash, E. *J. Biol. Chem.* **1981**, *256*, 6556−6564.

0002-7863/95/1517-9033$09.00/0

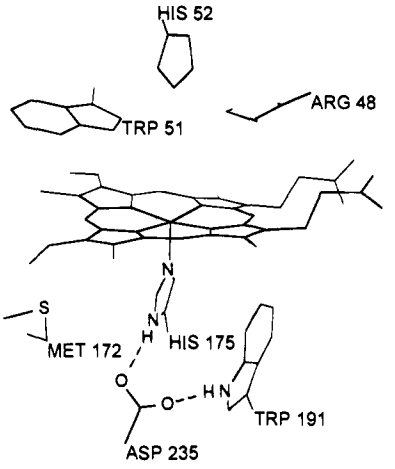

Figure 1. Crystal structure of the active site of cytochrome *c* peroxidase compound ES showing the heme macrocycle, the proximal His-175 which ligates the Fe, the site of the radical Trp-191, and two sites earlier proposed as radical sites, Trp-51 and Met-172. Asp-235 forms a hydrogen bond link between His-175 and Trp-191.

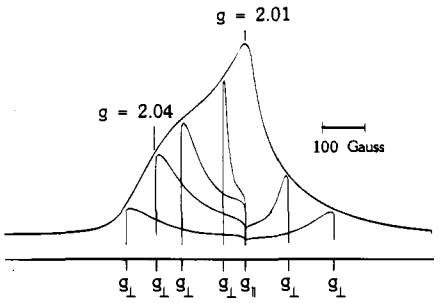

Figure 2. Dispersion rapid-passage EPR spectrum of compound ES. Within the EPR envelope are sketches representative of component EPR signals from molecules with different δ. Conditions: microwave power, 2mW; modulation amplitude, 0.67 G; sweep rate, 4.2 G/s; time constant, 0.032 s; microwave frequency: 35.18 GHz.

site.[13-15] The mutant, Trp-191 → Phe, did show a significantly altered EPR signal.[16,17] Unfortunately, mutagenesis examines residues by replacing them, and it is never certain whether a change in properties results from a mutation at the active site, or whether it merely is the indirect consequence. Hence, site-directed mutagenesis is only able to *eliminate* possible sites, but it cannot definitively *identify* a site. Studies done by X-ray crystallography of CcP compound ES were also unable to identify the location of the radical.[18,19] However, the cloning of CcP permits the preparation of unperturbed CcP that is isotopically enriched at specific atoms within particular amino acid types. Electron nuclear double resonance spectroscopy (ENDOR) of labeled compound ES provides the means to identify the radical of the enzyme in this unperturbed state. Preliminary measurements on uniformly ^{2}H-labeled native and mutant proteins showed[20,21] that the radical species was definitely a Trp residue and was almost certainly Trp-191.[22]

In light of this identification, the breadth of the EPR spectrum observed for this unusual protein free radical is indeed anomalous. Consequently, we recently reexamined the compound ES EPR spectrum, and found that it is not associated with the isolated $S^R = 1/2$ Trp radical, but must be described in terms of a weak exchange interaction between the radical and the $S^{Fe} = 1$ [Fe(IV)=O] heme.[23] The exchange interaction leads to an axial **g** tensor with

$$g_{\|}^{ES} \approx g^R = 2.0$$

$$g_{\perp}^{ES} \approx g_{\|}^{ES} + 2g_{\perp}^{Fe}(J/D) \qquad (1)$$

$$\approx 2.0 + \delta$$

$$\delta \equiv 2g_{\perp}^{Fe}(J/D)$$

where $g_{\|}^{ES}$ for the spin-coupled system lies along the Fe=O bond, near the heme normal,[18] $g^R \approx 2.0$ is the g value of the isolated radical, $g_{\perp}^{Fe} \approx 2.25$ is the $g_{\perp}$ value for the isolated oxyferryl heme, J is the exchange constant, and D is the oxyferryl zero field splitting. Thus, each molecule has an axial **g** tensor with $g_{\|} = 2$ and $g_{\perp} = 2 + \delta$, where δ is proportional to the exchange interaction between the heme and the radical.[24,25] However, the observed EPR spectrum of frozen-solution compound ES is a superposition of contributions from molecules with a distribution in values of J and therefore $g_{\perp}$, as indicated in the drawing in Figure 2. The result is an EPR envelope whose maximum intensity comes at the common value of $g_{\|} \approx 2.0$, and whose intensity falls monotonically both to high and low g values. The shoulder at $g \approx 2.04$ (Figure 2) that gives rise to a "perpendicular" feature in the derivative spectrum[5] merely arises from an enhanced contribution to the distribution at this value of $g_{\perp}$.

Such a formal treatment is independent of and gives no information about the detailed properties of the radical involved. The present paper completes the ENDOR characterization of compound ES with experiments on enzyme labeled with ^{2}H at specific positions on Trp, with ^{15}N at N1 of the indole ring, and with ^{13}C at C2 of the ring and at Cβ of the side chain. The choice of isotopic labels was determined by two parallel approaches to the problem: (i) the effort to ascertain whether a strongly-coupled, exchangeable proton detected earlier[22] is associated with the Trp indole ring nitrogen, thus signifying the presence of the Trp cation radical, or whether it involves a C−H bond that becomes labilized in the radical state, as seen in the case of pyruvate formate-lyase,[7] and (ii) an attempt to determine the odd-electron spin densities on the indole ring, as guided by molecular orbital calculations showing that the two alternative indole π-radicals have quite different distributions of π-spin density (see Figure 3).[12,26] It is useful to emphasize that the goal of this study, to characterize a one-electron hole and to determine the location of a single proton, is totally beyond

(13) Goodin, D. B.; Mauk, A. G.; Smith, M. *Proc. Natl. Acad. Sci. U.S.A.* **1986**, *83*, 1295−1299.
(14) Fishel, L. A.; Farnum, M. F.; Mauro, J. M.; Miller, M. A.; Kraut, J.; Liu, Y.; Tan, X.; Scholes, C. P. *Biochemistry* **1991**, *30*, 1986−1996.
(15) Goodin, D. B.; Mauk, A. G.; Smith, M. *J. Biol. Chem.* **1987**, *262*, 7719−7724.
(16) Mauro, J. M.; Fishel, L. A.; Hazzard, J. T.; Meyer, T. E.; Tollin, G.; Cusanovich, M. A.; Kraut, J. *Biochemistry* **1988**, *27*, 6243−6256.
(17) Scholes, C. P.; Liu, Y.; Fishel, L. A.; Farnum, M. F.; Mauro, J. M.; Kraut, J. *Isr. J. Chem.* **1989**, *29*, 85−92.
(18) Edwards, S. L.; Xuong, N. H.; Hamlin, R. C.; Kraut, J. *Biochemistry* **1987**, *26*, 1503−1511.
(19) Fulop, V.; Phizackerley, R. P.; Soltis, S. M.; Clifton, I. J.; Wakatsuki, S.; Erman, J.; Hajdu, J.; Edwards, S. L. *Structure* **1994**, *2*, 201−208.
(20) Hoffman, B. M. *Acc. Chem. Res.* **1991**, *24*, 164−170.
(21) Hoffman, B. M.; DeRose, V. J.; Doan, P. E.; Gurbiel, R. J.; Houseman, A. L. P.; Telser, J. In EMR of Paramagnetic Molecules. In *Biological Magnetic Resonance 13*; Berliner, L. J.; Reuben, J., Eds.; Plenum Press: New York, 1993; pp 151−218.
(22) Sivaraja, M.; Goodin, D. B.; Smith, M.; Hoffman, B. M. *Science* **1989**, *245*, 738−740.
(23) Houseman, A. L. P.; Doan, P. E.; Goodin, D. B.; Hoffman, B. M. *Biochemistry* **1993**, *32*, 4430−4443.
(24) Schulz, C. E.; Devaney, P. W.; Winkler, H.; Debrunner, P. G.; Doan, N.; Chiang, R.; Rutter, R.; Hager, L. P. *FEBS Lett.* **1979**, *103*, 102−105.
(25) The exchange interaction is given by $H_{ex} = -JS^{Fe} \cdot S^R$ which is the same notation used in Schulz *et al.* (ref 24).
(26) Krauss, M.; Garmer, D. R. *J. Phys. Chem.* **1993**, *97*, 831−836.

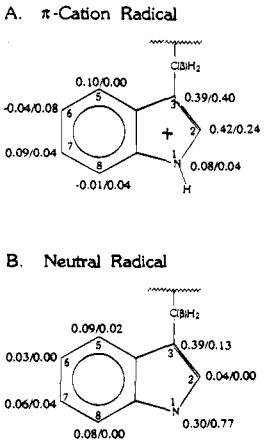

Figure 3. Predicted spin densities from cation and neutral radical tryptophans according to Hückel–McLachlan (HM)[12] and *ab initio*[26] calculations (KG). The numbering scheme is that used in the former paper. Densities are presented as HM/KG.

Table 1. Specifically Labeled and Unlabeled Samples of CcP[a]

designation	characteristics[b]
ES(H_8,H)	*b*; in H_2O
ES(H_8,D)	*b*; exchanged into D_2O
ES(D_5,H)	grown on DL-tryptophan-d_5 (ring deuterated); in H_2O
ES(D_5,D)	grown on DL-tryptophan-d_5 (ring deuterated); in D_2O
ES(D_8,H)	grown on DL-tryptophan-d_8 in H_2O
ES(D_8,D)	grown on DL-tryptophan-d_8 in D_2O
ES(^{15}N1)	grown on DL-tryptophan-$^{15}N1$
ES(^{13}C2)	grown on DL-tryptophan-^{13}C (ring C2 position)
ES($^{13}C\beta$)	grown on DL-tryptophan-$^{13}C\beta$
ES(C2D)	deuterated at C2H and partially along the ring in H_2O

[a] All samples are CcP(MKT) and are in H_2O and D_2O buffer as indicated. [b] Samples ES(H_8,H) and ES(H_8,D) are enzyme in natural isotopic abundance. All other samples are from the tryptophan auxotroph.

the resolution of X-ray crystallography and can only be reached spectroscopically.

ENDOR studies of an organic radical can identify exchangeable protons and yield spin density values through analysis of the hyperfine coupling tensors associated with nuclei at specific molecular sites. For a typical radical the ENDOR spectrum of a frozen solution is a "powder average" because the **g** anisotropy is small, and hyperfine tensors are obtained readily in principle.[27] Likewise, for paramagnetic centers with appreciable **g** anisotropy, these hyperfine tensors normally can be determined by relating ENDOR spectra taken at numerous fields across the EPR envelope to the corresponding subsets of molecular orientations that give rise to those spectra.[20,21] However, the fact that the EPR spectrum of compound ES arises from a distribution in the exchange coupling between the $S = 1$ (Fe=O) heme and the $S = 1/2$ Trp radical introduces considerable **g** anisotropy yet destroys the normal correspondence of the ENDOR field of observation with a well-defined subset of molecular orientations. Nonetheless, a limited correspondence remains. We have exploited this correspondence to prove the assignment of an indole π-cation radical and to obtain the spin densities around the indole ring of the radical.

Materials and Methods

Samples with six different isotopic labeling patterns were employed as listed in Table 1. Labeled CcP and mutants were expressed and purified from *Escherichia coli* HB2151 or amino acid auxotrophs as previously described.[28] Protein was expressed under control of the lac promoter in plasmid pLacCcP2-8. Specific amino acid labeling to produce CcP(Trp-d_5) and CcP(Trp-d_8) was done by expression in the *E. coli* tryptophan auxotroph JA300 grown in YNA media containing added amino acids as previously described.[22] CcP([^{13}C2]Trp), CcP([$^{13}C\beta$]Trp), CcP([C2D]Trp) and CcP([^{15}N1]Trp) were expressed from strain JA300 by an alternate method in which the cells in a 100 mL culture were switched from growth in a rich medium (YT + 100 μg/mL ampicillin) into a defined medium containing, per liter, 1x M9 salts, 1 mL of glycerol, 0.1 mM $CaCl_2$, 1 mM $MgSO_4$, 0.001% thiamine, 100 μg/mL ampicillin, and 1 g of each amino acid except Gln, Asn, Cys, Trp, and Gly, and finally containing 0.1–0.25 g of labeled Trp. The medium switch occurred in the late-log phase of growth, but before the expression of CcP occurred due to release of catabolite repression. This was confirmed by sodium dodecyl sulfate–polyacrylamide gel electrophoresis (SDS–PAGE) electrophoresis at the time of the switch. Expression in the defined medium was induced by 0.1 mM isopropyl β-thiogalactopyranoside for 12 h at 37 °C before cell harvest and purification. The extent of isotope incorporation was estimated in some samples by spiking the tryptophan to a known specific activity with tritiated Trp. The extent of labeling by perdeuterated CcP was estimated by determining the mass of the protein to within ±5 amu by electrospray mass spectroscopy. We observed that the labeling efficiency ranged from 40% to 85% for the deuterated Trp samples. L-Tryptophan-2′,5′,6′,7′,8′-d_5 (98.5%) (Trp-d_5),[29] DL-tryptophan-d_8 (98.6%) (Trp-d_8), and DL-tryptophan-1-^{15}N (99%) ([^{15}N1]Trp) were obtained from MSD Isotopes, Montreal, Canada. L-Tryptophan-2-^{13}C and L-tryptophan-β-^{13}C were obtained from the NIH Stable Isotope Resource, Los Alamos, NM. L-Tryptophan labeled predominantly at the C2 proton was made by acid labilized exchange.[30] L-Tryptophan was exchanged by refluxing in 0.2 M DCL/D_2O (99.5% D) under argon. Samples taken at various times were examined by NMR to monitor the extent of H/D exchange. After 4 h, the percentages of deuteration at the C2, C5, C6, C7, and C8 ring positions were 91%, 28%, 64%, 37%, and 43%, respectively. The sample was neutralized, evaporated to dryness, and recrystallized from H_2O/MeOH.

Continuous wave (CW) 35 GHz EPR and ENDOR spectra were taken at 2 K using equipment and procedures described previously.[31] Some ENDOR spectra were taken with broad-band radio frequency (rf) produced by mixing the output of a PTS 160 synthesizer with a Gaussian white noise source (100 kHz width) as described recently.[32] Mims ^{2}H pulsed 9 GHz[33] and 35 GHz ENDOR spectra were taken on instruments described elsewhere.[34,35]

The first-order ENDOR spectrum for a single orientation of a paramagnetic center that contains a nucleus of spin I has transitions at frequencies given by eq 2, where A_N and P_N are the angle-dependent

$$\nu_{\pm} = |\nu_N \pm A_N/2 + 3P_N(2m - 1)| \qquad (2)$$

hyperfine and quadrupole constants of nucleus N, respectively, $-m_I + 1 \leq m \leq m_I$, and ν_N is the nuclear Larmor frequency.[36] For ^{2}H ($I = 1$) at 35 GHz, $\nu_N > A_N > P_N$, and eq 2 describes a Larmor-split doublet centered at ν_N with lines at frequencies of $\nu_N \pm A_N/2$ and possibly

(27) Hoganson, C. W.; Babcock, G. T. *Biochemistry* **1992**, *31*, 11874–11880.

(28) Goodin, D. B.; Davidson, M. G.; Roe, J. A.; Mauk, A. G.; Smith, M. *Biochemistry* **1991**, *30*, 4953–4962.

(29) The tryptophan numbering scheme used in this paper is consistent with that used in Hoffman *et al.* (ref 12). This scheme is different from that used in Krauss and Garmer (ref 26), and in order to make direct comparisons between the two sets of data, the Krauss and Garmer numbers have been adapted so they correspond to the same place on the Trp.

(30) Kim, S.-T.; Sancar, A.; Essenmacher, C.; Babcock, G. T. *Proc. Natl. Acad. Sci. U.S.A.* **1993**, *90*, 8023–8027.

(31) Werst, M. M.; Davoust, C. E.; Hoffman, B. M. *J. Am. Chem. Soc.* **1991**, *113*, 1533–1538.

(32) Hoffman, B. M.; DeRose, V. J.; Ong, J.-L.; Davoust, C. E. *J. Magn. Reson., Ser. A* **1994**, *110*, 52–57.

(33) Fan, C.; Kennedy, M. C.; Beinert, H.; Hoffman, B. M. *J. Am. Chem. Soc.* **1992**, *114*, 374–375.

(34) Fan, C.; Doan, P. E.; Davoust, C. E.; Hoffman, B. M. *J. Magn. Reson.* **1992**, *98*, 62–72.

(35) Davoust, C. E.; Doan, P. E.; Hoffman, B. M. *J. Magn. Reson.*, submitted for publication.

(36) Abragam, A.; Bleaney, B. *Electron Paramagnetic Resonance of Transition Ions*, 2nd ed.; Clarendon Press: Oxford, 1970.

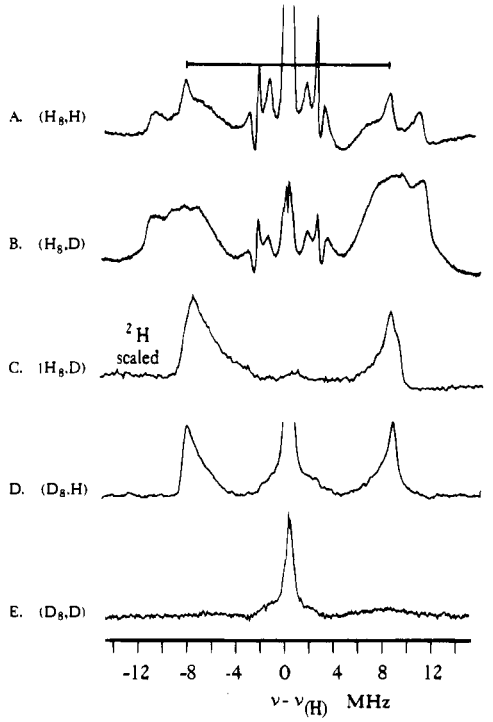

Figure 4. ^1H and ^2H ENDOR of native and exchangeable ^1H: (A) ^1H ENDOR of ES(H_8,H); (B) ^1H ENDOR of ES(H_8,D); (C) ^2H pulsed ENDOR of ES(H_8,D); (D) ^1H ENDOR of ES(D_8,H); (E) ^1H ENDOR of ES(D_8,D). Conditions (A, B, D, E): (CW ENDOR) microwave frequencies between 35.09 and 35.0 GHz; microwave power, (A) 0.23, (B) 1.82, (D) and (E) 5 mW; modulation amplitude, (A and B) 0.16, (D and E) 1.06 G; scan rate, (A and B) 0.5, (D) 2, (E) 1 MHz/s; number of scans, (A) 36, (B) 50, (D) 200, (E) 325. All spectra taken with 20 W rf power and at 2 K. Conditions (C): (Q-band Mims ENDOR) microwave frequency 34.75 GHz, magnetic field, 12400 G, $\pi/2$ pulse width 100 ns, $\tau_{12} = 200$ ns, $\tau_{rf} = 70$ μs (73 400 ns); repetition rate, 25 ms; no transients/pt; 256 pts/spectrum; $T = 2$ K.

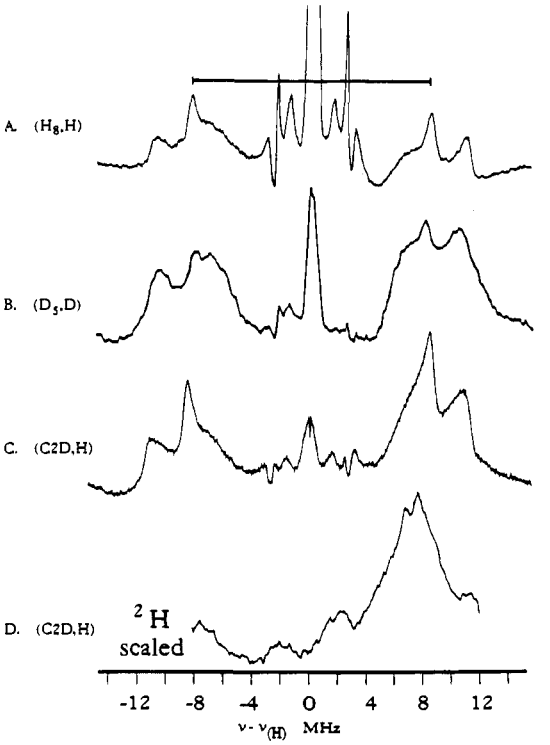

Figure 5. ^1H ENDOR and ^2H ENDOR of nonring and ring ^1H: (A)^1H ENDOR of ES(H_8,H), reproduced here from Figure 4 for convenience; (B) ^1H ENDOR of ES(D_5,H); (C) ^1H ENDOR of ES(C2D, H); (D) ^2H pulsed ENDOR of ES(C2D, H). Conditions: (CW) (A) same as in Figure 4A; microwave frequency, (B), 35.30, (C) 35.18 GHz; microwave power, (B) 5, (C) 0.91 mW; modulation amplitude, (B) 1.06, (C) 0.16 G; scan rate, (B) 2, (C) 0.5 MHz/s; number of scans, (B) 100, (C) 70; rf power, 20 W; (Mims pulsed) (D) microwave frequency, 9.56 GHz; magnetic field, 3380 G; $\pi/2$ pulse width, 60 ns; $\tau_{12} = 244$ ns; $\tau_{rf} = 67$ μs; repetition rate, 20 ms; 234 transients/pt; 256 pts/spectrum; $T = 2$ K.

split further by the quadrupole term. For the $I = 1/2$ nuclei, ^1H, ^{13}C, and ^{15}N, the quadrupole term is absent. In the case of ^1H, the ENDOR pattern is centered at ν_H and split by A_H. For ^{15}N and ^{13}C, however, the spectrum may be centered either at $A_N/2$ or at ν_N, whichever is larger, and split by A_N or $2\nu_N$, whichever is smaller. The hyperfine constants of $^1H/^2H$ and $^{14}N/^{15}N$ are related by the expressions

$$A(^1H)/A(^2H) = \nu(^1H)/\nu(^2H) = 6.5 \quad (3)$$

$$A(^{15}N)/A(^{14}N) = \nu(^{15}N)/\nu(^{14}N) = 1.4 \quad (4)$$

A CW ENDOR spectrum usually shifts in frequency in the direction of the scan. This sweep effect reflects details of spin relaxation that are not of concern here.

Results

ENDOR spectra have been recorded for compound ES prepared from Trp that had been isotopically labeled with ^{13}C, ^{15}N, and ^2H. Representative spectra taken at the peak of the EPR signal, near $g = 2.01$, are presented in Figures 4–7.

Figure 4 shows the $^{1,2}H$ spectra. Figure 4A is a ^1H ENDOR spectrum of compound ES in natural ^1H isotopic abundance in H_2O buffer (ES(H_8,H); $g = 2.00$). The spectrum is roughly symmetric about the proton Larmor frequency, $\nu(^1H) \approx 53$ MHz, and numerous local ENDOR doublets (eq 2) with hyperfine couplings in the range from $1 \leq A(^1H) \leq 21$ MHz, along with a distant ^1H ENDOR peak at $\nu(^1H)$. Figure 4B is of the native protein in D_2O (ES(H_8,D)); although the spectral features in parts A and B of Figure 4 are quite similar, we note in the D_2O sample a reduced intensity for the distant ENDOR peak at

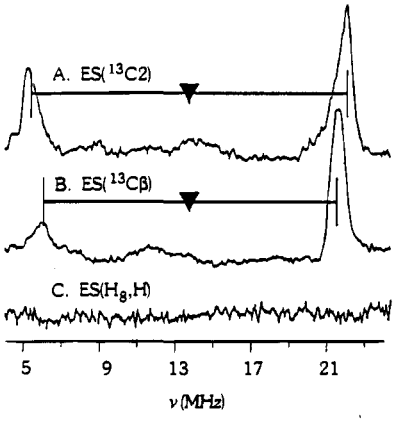

Figure 6. ^{13}C ENDOR spectrum of ES. (A) ES($^{13}C2$); (B) ES($^{13}C\beta$); (C) ES(H^8,H). All spectra were taken with 5 mW microwave power, 0.67 G modulation amplitude, 1 MHz/s scan rate, 0.032 s time constant, and 20 W rf power using a low-pass rf filter. Conditions: (A) ($^{13}C2$) microwave frequency, 35.46 GHz; $g = 1.994$; 500 scans; no noise source; (B) ($^{13}C\beta$) microwave frequency, 35.21 GHz; $g = 1.994$; 35 scans; noise source; (C) microwave frequency, 35.47 GHz; $g = 1.994$; 50 scans; no noise source. No ^{14}N resonances appear for the unlabeled sample because such resonances are much weaker and not enough scans were signal-averaged for ^{14}N peaks to appear.

$\nu(^1H)$ and also reduced intensity for the sharp $A(^1H) \approx 16$ MHz doublet as compared to the H_2O sample. Q-band pulsed ^2H spectra of ES(H_8,D) (Figure 4C; scaled by the nuclear g factor, eq 3) exhibit a well-resolved doublet that confirms the presence of an exchangeable proton/deuteron with $A(^1H) = 16$ MHz. The

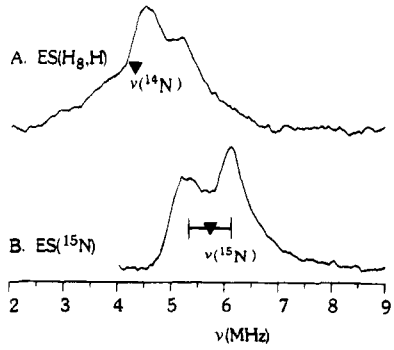

Figure 7. ^{15}N and ^{14}N ENDOR spectrum of ES. (A) ES(H^8,H); (B) ES(^{15}N) Conditions: spectra taken with 5 mW microwave power, 0.67 G modulation amplitude, 1 MHz/s scan rate, 0.032 s time constant, and 20 W rf power using a low-pass rf filter; (A) microwave frequency, 35.04 GHz; g = 2.00; 200 scans; noise source; (B) microwave frequency, 35.39 GHz, g = 2.00; 250 scans.

spectrum of ES(D_8,H), Figure 4D, shows that deuteration of the tryptophan constitutive proton sites suppresses all proton signals with the exception of the distant ENDOR signals near $\nu(^1H)$ and the sharp doublet with A = 16 MHz. Subjecting this perdeuterated enzyme sample to H/D exchange eliminates this doublet (sample ES(D_8,D); Figure 4E), showing that it is associated with the exchangeable proton suggested by the loss of the ^1H intensity in Figure 4B and proven by the appearance of the ^2H doublet in Figure 4C. The combined $^1H/^2H$ ENDOR results definitely identify the radical site of ES as tryptophan, with no appreciable amounts of spin density delocalized to other residues. They also show the presence of a strongly-coupled exchangeable proton. With the radical site thus proven to be a Trp, the identification as Trp-191 follows from earlier arguments.[22]

The obvious assignment of the exchangeable proton with $A(H) \approx 16$ MHz is to the N1H proton of a Trp cation radical. However, Krauss and Garmer concluded that ES contains a Trp neutral radical, with the N1 site unprotonated,[26] which is in disagreement with this assignment. In addition, ^{15}N ENDOR data, which would be definitive in assessing the spin density at the N1 site of an isolated radical, turns out to be equivocal in the exchange-coupled center of ES (*vide infra*). It is also known that radical formation can labilize otherwise nonexchangeable protons[7] and the C2 proton on the Trp indole ring is a plausible candidate for such labilization. Thus, additional ENDOR data were collected for other deuterium labeling patterns (Table 1 plus Figure 5) to distinguish between ring and side chain protons of the Trp and to identify the exchangeable 16 MHz proton.

In the proton spectrum of a sample containing ring-deuterated Trp that was exchanged into D_2O (ES(D_5,D); Figure 5B), the ^1H signals from exchangeable ^1H and the constitutive ring protons are eliminated. The spectrum consists of two distinct hyperfine-split doublets that are assigned to the two $C\beta H_2$ protons; one has A = 13 MHz, and the other has A = 21 MHz.

To test whether the exchangeable proton with A = 16 MHz was associated with the Trp C2H proton that has been labilized in the radical state, a sample was prepared in which ring protons on Trp were partially deuterated; compound ES(C2D,H) contains 90% deuteration at C2 and partial deuteration at other ring positions (see Materials and Methods). This sample was used to collect the bottom two spectra of the figure, with Figure 5C being a proton spectrum and Figure 5D an X-band Mims deuteron spectrum (scaled by the nuclear g factor, eq 3). Comparison of Figure 5C with the spectrum of ES in natural ^1H isotopic abundance (ES(H_8,H), included as Figure 5A) shows that the deuteration causes numerous changes throughout the ^1H envelope, such that no simple interpretation is possible. However, the scaled ^2H ENDOR of the partially deuterated sample ES(C2D,H) clearly shows the ν_+ feature of a doublet with $A(^2H) \approx 2.3$ MHz, corresponding to $A(^1H) \approx 15$ MHz, along with a 0.8 MHz deuteron coupling that corresponds to a proton with $A(^1H)$ = 5 MHz. Because the sample is dissolved in H_2O buffer, these deuterons must be associated with a nonexchangeable constitutive site on the ring. Given the theoretical calculations of spin densities (Figure 3)[12,26] and the extent of exchange at the various sites, the nonexchangeable deuteron/proton with $A \approx 15$ MHz must be attached to the C2 carbon. On the basis of the degree of exchange, the deuteron/proton with $A(^2H) \approx 0.8$ MHz ($A(^1H) \approx 5$ MHz) can be assigned to the α-proton of C6 on the six-membered ring.

These results leave little doubt that the exchangeable proton with $A \approx 16$ MHz must be associated with the indole nitrogen. The further determination of the degree to which the radical is a simple Trp cation radical with protonated NH, as opposed to the possibility of partial deprotonation through interaction with the carboxylate of Asp-235, has been addressed by detailed investigation of the spin density distribution on the indole ring.

As part of the effort to determine the spin density distribution, studies were done with Trp specifically labeled with ^{13}C at C2 and at Cβ and with ^{15}N label at N1. (Of course, the appearance of ^{13}C and ^{15}N resonances from samples prepared with isotopically labeled Trp is yet another illustration that Trp is the site of the radical.) Figure 6 presents the ^{13}C ENDOR spectrum of ES grown from Trp selectively labeled at the C2 position (ES-($^{13}C2$); Figure 6A) of the indole ring and at the Cβ position (Figure 6B) of the side chain, ES($^{13}C2$). The former spectrum shows two ^{13}C peaks at 5 and 21.5 MHz that are absent in the natural-abundance ENDOR spectrum (Figure 6C) and that correspond to a hyperfine-split $\nu_\pm$ doublet centered at $\nu(^{13}C)$ = 13.2 MHz, with $A(^{13}C2)$ = 16 MHz. The $^{13}C\beta$ spectrum from ES($^{13}C\beta$) also shows a $\nu_\pm$ doublet at 5.5 and 21 MHz, centered at $\nu(^{13}C)$ = 13.1 MHz with hyperfine coupling, $A(^{13}C\beta)$ = 15 MHz. Although these two couplings fortuitously are quite similar, NMR spectra of the ^{13}C-labeled Trp precursors confirm the identity of the labeling site ($\sigma(^{13}C2) \approx 120$ ppm, $\sigma(^{13}C\beta) \approx 24$ ppm) and numerous spectra show that these ENDOR frequencies are reproducibly different.

Figure 7A shows that the nitrogen ENDOR of ES for a natural-abundance sample (^{14}N) changes with the ^{15}N-labeled tryptophan. The spectrum of the ^{14}N sample (Figure 7A) shows the ν_+ branch of a ^{14}N pattern split by a hyperfine coupling of $A(^{14}N) \approx 0.6$ MHz; frequently the ν_- branch is weak in Q-band ENDOR. It is shifted off the ^{14}N nuclear Larmor frequency (3.8 MHz) by 0.4 MHz due to the sweep effect (see Materials and Methods). The spectrum of ^{15}N-labeled protein (Figure 7B) shows both the $\nu_\pm(^{15}N)$ branches split by $A(^{15}N) \approx 0.8$ MHz, corresponding to the value expected from the ratio of nuclear g factors; the center of the pattern is shifted by the sweep effect by 0.4 MHz.

Analysis

Conformation of the Trp Radical. According to molecular orbital calculations[12,26] both cationic and neutral forms of a Trp radical are expected to have large spin density at C3 (Figure 3). Analysis of the observed hyperfine coupling to the protons on Cβ thus cannot help in distinguishing between these two possibilities, but it can be used as a check on the MO calculations and, even more important, as a check on the consistency of the ENDOR data with the known X-ray structure of compound ES.[10] The hyperfine interaction for protons on an aliphatic carbon attached to an aromatic π system is

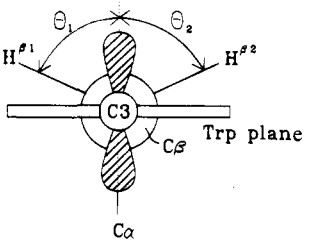

Figure 8. Newman projection looking down the C3−Cβ bond from C3 of the Trp plane. θ_1 is defined as the dihedral angle from the p-orbital to $CH^{\beta 1}$.

effectively isotropic.[37] It is proportional to the spin density on the adjacent trigonal carbon of the ring, in this case $\varrho^{\pi}(C3)$, and to a trigonometric factor that depends on the dihedral angle between the Cβ−H bond and the p-orbital of the C3 ring carbon:[37]

$$A(^1H^{\beta 1}) = [B_0 + B_2 \cos^2 \theta_1]\varrho^{\pi}(C3) \approx [B_2 \cos^2 \theta_1]\varrho^{\pi}(C3) \quad (5)$$

$$A(^1H^{\beta 2}) = [B_0\ B_2 \cos^2 \theta_2]\varrho^{\pi}(C3) \approx [B_2 \cos^2(\theta_1 + 2\pi/3)]\varrho^{\pi}(C3)$$

The first term in the brackets, B_0, is a negligible constant; the second term arises from hyperconjugation with the π-orbital to the β-protons and is characterized by $B_2 \approx 162$ MHz.[38] In eq 5 we have assumed idealized geometries, assigning θ_1 to $^1H^{\beta 1}$, and taking $\theta_2 = \theta_1 + 120°$ for $^1H^{\beta 2}$ (Figure 8).

Because a β-proton coupling *is* isotropic and thus independent of the molecular orientation with respect to the external field, the $-CH_2-$ coupling can be determined from an ENDOR spectrum associated with any molecular orientation. Thus, in this case the distribution in exchange couplings does not introduce the difficulties mentioned in the Introduction. Through the use of eq 5 and the experimentally determined hyperfine couplings, $A^1 \approx 21$ MHz and $A^2 \approx 13$ MHz (Figure 6C), we obtain $\theta_1 \approx -56°$ for the dihedral angle experiments in complete agreement with $\theta = -54.6°$ as obtained from the X-ray structure. The experimentally determined value for the spin density is $\varrho^{\pi}(C3) \approx 0.41$, which also compares exceptionally well with the Hückel−McLachlan calculation for either the neutral or the cation radical (Figure 3). The *ab initio* calculation of Krauss and Garmer[26] actually predicts a difference in spin density at the C3 position for the two aromatic radicals; the neutral radical should have only 13% spin density at C3 as opposed to 40% for the cationic radical. Although this calculation likely overestimates the difference, the experimental spin density on C3 appears to lend support to the assignment as a cation radical.

The observation of ^{13}C hyperfine coupling on Cβ provides an independent check of the spin density on C3. We calibrate the coupling of a ^{13}C attached to a trigonal carbon by comparison to the ^{13}C hyperfine coupling to the ethyl radical, $^{\bullet}C1H_2-{}^{13}C2H_3$, where $\varrho^{\pi}(C1) \approx 1$ and $A(^{13}C2) \approx 39$ MHz is isotropic.[39] By comparison the observed $^{13}C\beta$ coupling of 15 MHz corresponds to a spin density of $\varrho^{\pi}(C3) = 0.38$ on C3 which is in agreement with $\varrho^{\pi}(C3)$ from the Hβ data. However, we prefer the value from the proton data (0.41) for inclusion in the summary, Figure 9.

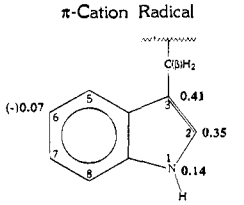

Figure 9. Experimentally determined spin densities on the Trp 191 π-cation radical. The negative sign for C6 was taken from the Hückel−McLachlan calculation. The uncertainties in these values are discussed in Appendix II.

^{13}C and $^{14,15}N$ ENDOR. Both semiempirical and *ab initio* calculations on indole π-radicals indicate that[12] the spin densities at C2 and N1 differ greatly between the cation radical and the neutral radical (Table 1). Thus, we collected ^{13}C and $^{14,15}N$ ENDOR spectra from ES($^{13}C2$), the unlabeled enzyme, and ES-($^{15}N1$) in hopes of obtaining the hyperfine tensors, and using them to calculate the spin densities of the atoms directly. In general, the full hyperfine tensors for a frozen solution can be determined from measurements made at multiple fields.[20,21] Unfortunately, as explained in Appendix I, the distribution in $g_{\perp}$ makes this impossible.

Spin Densities of C2, N1, and C6. Fortunately, the spin densities of C2, N1, and also C6 can be calculated from the ^1H hyperfine couplings measured at $g = 2.01$ for the α-protons attached to those atoms; using the following method, full determination of the hyperfine tensors is not needed. The ^1H hyperfine tensor for the *i*th α-proton (i = H1, H2) can be written in terms of the π-spin density on the atom to which it is attached, $\varrho^{\pi}(j)$ (j = N1, C2, C3), and the local hyperfine interaction matrix for unit spin on that atom, $\mathbf{A}^j$, along with terms that take into account through-space dipolar couplings to those nearby ring atoms, *i*, that have a significant spin density.[40] The latter terms are proportional to the spin density on the neighbor $\varrho^{\pi}(j)$ and the dipolar coupling matrix for unit spin on that neighbor $\mathbf{T}^i_j$, which can be calculated according to McConnell and Strathdee[41] or approximated as a point dipole.[40] In the case of the C2 or the N1 protons, the hyperfine couplings would be described as

$$\mathbf{A}(H2)_{tot} = \mathbf{A}^{C2}\varrho^{\pi}(C2) + \mathbf{T}^{H2}{}_{N1}\varrho^{\pi}(N1) + \mathbf{T}^{H2}{}_{C3}\varrho^{\pi}(C3) \quad (6a)$$

$$\mathbf{A}(H1)_{tot} = \mathbf{A}^{N1}\varrho^{\pi}(N1) + \mathbf{T}^{H1}{}_{C2}\varrho^{\pi}(C2) + \mathbf{T}^{H1}{}_{C3}\varrho^{\pi}(C3) \quad (6b)$$

The results from the use of these equations (Appendix II) show that contributions from spin densities on the other ring atoms are so low that it is unnecessary to consider dipolar couplings with them. Thus, the only unknown quantities on the right-hand side of eqs 6a and 6b are the three spin densities; this reduces to two because it was found above that $\varrho^{\pi}(C3) = 0.41$. (Again, contribution from spin density on C2 and N1 can be neglected when determining $\varrho^{\pi}(C3)$ from Hβ couplings.) As a result, if hyperfine couplings for H1 and H2 are available for even one known orientation of the field with respect to the molecular frame (single-crystal orientation), eqs 6a and b can be incorporated into the well-known equation for orientation-dependent hyperfine couplings (Appendix II) to calculate the two spin densities $\varrho^{\pi}(N1)$ and $\varrho^{\pi}(C2)$.

Following our model for distributed spin coupling between the oxyferryl heme an the Trp-191 radical, the measured couplings at $g = 2.01$ in fact arise from molecules with a single

(37) Carrington, A.; McLachlan, A. D. *Introduction to magnetic resonance with applications to chemistry and chemical physics*; Harper & Row: New York, 1967.

(38) Bender, C. J.; Sahlin, M.; Babcock, G. T.; Barry, B. A.; Chandrashekar, T. K.; Salowe, S. P.; Stubbe, J.; Lindström, B.; Petersson, L.; Ehrenberg, A.; Sjöberg, B.-M. *J. Am. Chem. Soc.* **1989**, *111*, 8076−8083.

(39) Bolton, J. R. In *Radical Ions*; Kaiser, E. T., Kevan, L., Eds.; Interscience Publishers: New York, 1968; pp 1−34.

(40) O'Malley, W. H. O.; Babcock, G. T. *J. Am. Chem. Soc.* **1986**, *108*, 3995−4001.

(41) McConnell, H. M.; Strathdee, J. *Mol. Phys.* **1959**, *2*, 129−138.

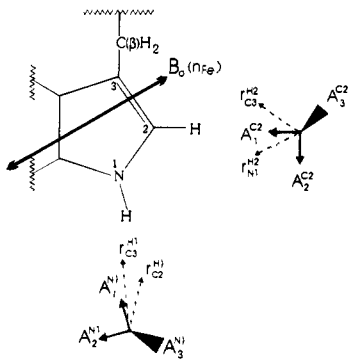

Figure 10. Orientation of Trp 191 in the magnetic field with relative tensors defined. Orientation is given of the magnetic field for all molecules at $g = 2.01$, where $\mathbf{B}_0$ lies along the heme normal ($\mathbf{n}^{Fe}$). Numbering and orientation of hyperfine tensors at H1 and H2 are indicated as discussed in Appendix II.

orientation: the field is normal to the heme plane and lies roughly in the indole plane of Trp-191 as shown in Figure 10. Thus, the available ENDOR data for H1 and H2 are sufficient for a calculation of the desired spin densities; this novel procedure is described in Appendix II. The final values are $\varrho^{\pi}(C2) = 0.35$ and $\varrho^{\pi}(N1) = 0.14$. As seen by comparing calculated spin densities[12,26] (Figure 3) for N1, C2, and C3 with the experimental ones (Figure 9), this result clearly confirms the presence of the Trp cation radical.

The spin density on C6 likewise can be estimated from the measured coupling constant, but here it is necessary to consider only the local term ($\mathbf{A}^i$) for an α-proton attached to a carbon atom (eq A3a; see Appendix I). The contributions from spin density on neighboring atoms can be neglected because in either form of the radical, these ring atoms show very little spin density and their contributions from the point dipole approximation would be not be detected within the accuracy of the calculation. The hyperfine coupling constant of $A(^1H6) = 5$ MHz corresponds to a spin density of $\varrho^{\pi}(C6) = (-)0.07$, where the sign is chosen to correspond with the prediction of the Hückel–McLachlan calculation (Figure 3).

Discussion

The study of compound ES demonstrates the power of Q-band CW and pulsed ENDOR coupled with specific isotopic labeling of amino acids to identify and characterize the radical site of an enzyme. The ENDOR spectra of perdeuterated Trp, ^{13}C-labeled Trp, and ^{15}N-labeled Trp prove that the radical is on a Trp, and a variety of arguments show that it must be Trp-191.[42] The present study has completed the investigation by determining the radical's protonation state and its spin density distribution.

The observation of an exchangeable proton associated with the radical would appear to straightforwardly indicate that it is the π-cation radical protonated at N1, which should be a position of low spin density (Figure 3). However, such an assignment required verification because of the absence of a clear correspondence between the observed nitrogen coupling and the exchangeable proton coupling, and in light of the study of pyruvate formate-lyase, which shows that normally exchange-inert protons can be labilized in a radical.[7] The C2 proton of the indole ring is a candidate for such labilization, but the pulsed ^{2}H ENDOR spectrum of ES prepared with selectively deuterated Trp shows that it does not exchange. Thus, the assignment of the exchangeable proton to N1 is correct: ES indeed contains the Trp π-cation radical. Such is also the case in DNA photolyase,[8] the second enzyme found to use tryptophan oxidation in its mechanism of function.

The direct proof by ENDOR spectroscopy that ES contains a Trp cation radical, presumably interacting with the carboxylate of Asp-235, is in disagreement with the conclusion of Krauss and Garmer, based on detailed calculations of optical spectra, that ES contains the Trp neutral radical, interacting with the neutral Asp-235 carboxyl group. Given that the magnetic resonance measurements are all done at helium temperature and the optical spectroscopy at ambient temperature, it is conceivable that each conclusion is correct for its respective conditions. However, it does not seem plausible to us that charge separation could be absent at high temperature yet develop at low temperature, where dielectric constants are reduced. Thus, we propose that the ENDOR assignment is valid at all temperatures. This proposal is in complete agreement with the recent report[43] which shows that the cavity created by mutagenic removal of Trp-191 will specifically bind heterocyclic compounds only if they are cations.

Through a combination of ^{13}C and ^{2}H labeling, we have determined the hyperfine couplings at $g = 2.01$ for $^{13}C\beta$, and the $C\beta H_2$, N1, and C2H protons. These couplings have been analyzed within the model for the magnetic properties of the spin-coupled heme–radical redox cluster of ES. The resulting spin densities for the radical (Figure 9) are in remarkable agreement with those predicted for the cation radical by the semiempirical Hückel–McLachlan MO theory (Figure 3), which in turn are comparable to those of the *ab initio* calculation for this state. The spin densities are in total disagreement with values predicted for the neutral radical, thereby confirming the assignment as the cation radical and further suggesting that the cation radical is not significantly deprotonated by N1H···O hydrogen bonding to the carboxylate of Asp-235 and that the structure of ES in the vicinity of Trp-191 differs little from that of the resting state of the enzyme (Figure 1). Improved theoretical calculations on the radical will speak to this point.

In summary, this paper completes the characterization of the active site of compound ES as being composed of an oxyferryl heme coupled to the Trp-191 π-cation radical by a weak, distributive exchange coupling. It thereby provides the final piece to a puzzle first recognized over a quarter of a century ago.[5]

Acknowledgment. We thank Mr. Clarke E. Davoust for expert technical assistance, Dr. Stephen Kent for mass spectroscopic analyses, and Dr. J. A. Fee and the Stable Isotope Resources of Los Alamos National Laboratory, supported by USPHS Grant RR02231 and by the U.S. Department of Energy, for the labeled Trp. This work was supported by Research Grants NIH HI13531 to B.M.H. and GM41049 to D.B.G. and by NIH Training Grant 5 T32 GM0838205.

Appendix I

Analysis of Trp Indole ^{13}C and ^{14,15}N ENDOR. Consider hyperfine tensors for a nonhydrogenic atom of a π-radical, such as ^{13}C2 or ^{14,15}N of Trp, which have axial symmetry with $A_{||}$ (^{13}C and ^{14}N) lying perpendicular to the radical (indole) plane, a direction denoted $\mathbf{n}_{||}$. They can be written as[44]

(42) Lerch, K.; Mims, W. B.; Peisach, J. *J. Biol. Chem.* **1981**, *256*, 10088–10091.

(43) Fitzgerald, M. M.; Churchill, M. J.; McRee, D. E.; Goodin, D. B. *Biochemistry* **1994**, *33*, 3807–3818.

(44) Wertz, J. E.; Bolton, J. R. *Electron spin resonance: elementary theory and practical applications*, 2nd ed.; Chapman and Hall: New York, 1986.

$$\mathbf{A}(^{13}C2) = a(^{13}C2) + \mathbf{T}(C) \equiv [A_\perp, A_\perp, A_\parallel] \quad \text{(A1a)}$$

$$\mathbf{A}(^{14}N1) = a(^{14}N1) + \mathbf{T}(N) \equiv [A_\perp, A\perp, A_\parallel] \quad \text{(A1b)}$$

$$\mathbf{T}(C) = [-91, -91, +182]\varrho^\pi(C)\ \text{MHz}$$

$$\mathbf{T}(N) = [-48, -48, +98]\varrho^\pi(N)\ \text{MHz}$$

In the structure of CcP, the heme normal ($\mathbf{n}_{Fe}$) can be taken as perpendicular to $\mathbf{n}_I$, the normal to the plane of the indole ring: the deviation is only 8° ($\cos^{-1}(\mathbf{n}_I \cdot \mathbf{n}_{Fe}) = 82°$). This makes it straightforward to predict the field dependence of the ENDOR spectrum of a nucleus with an axial hyperfine tensor, (eq A1) for the spin-coupled center of compound ES, where the EPR envelope is determined by the distribution in J (eq 1). At all fields one expects to see a pattern composed of $\nu_\pm$ branches that are dominated by a doublet with the frequencies $(\nu_\pm)_\perp = \nu_n \pm A_\perp/2$. The pattern for each branch should fall off sharply in intensity as the frequency departs from $(\nu_\pm)_\perp$ and should extend to $(\nu_\pm)_\parallel = \nu_n \pm A_\parallel/2$, where it should exhibit a broad step. ^{13}C and $^{14,15}N$ ENDOR spectra collected at numerous fields across the EPR envelope all showed peaks indistinguishable from those presented in Figures 6 and 7. Considering the data for $^{13}C2$, Figure 6, the invariant hyperfine coupling constant observed for ^{13}C should correspond to $(\nu_\pm)_\perp$, giving $A_\perp(^{13}C2) \approx 15$ MHz. However, we were unsuccessful in detecting the shoulder that would correspond to $A_\parallel(^{13}C2)$; a similar result was found for $^{14,15}N$.

Unfortunately, it is not possible to calculate $\varrho^\pi(C2)$ or $\varrho^\pi(N1)$ knowing only $A_\perp$; one must determine T(C) and T(N), and this requires both $A_\perp$ and $A_\parallel$. The reason that only T is useful in determining ϱ^π is that T is directly proportional to the π-spin density on the corresponding atom (eq A1), whereas the isotropic coupling is a nonlocal property. For example, for C2 it depends on spin densities at N1, C2, and C3.[37]

$$a(^{13}C2) \approx (S^C + Q_{CN}{}^C + Q_{CH}{}^C + Q_{CC'}{}^C)\varrho^\pi{}_{C2} + Q_{NC}{}^C\varrho^\pi{}_{N1} + Q_{C'C}C\varrho^\pi{}_{C3} \quad \text{(A2)}$$

where the superscripts indicate the atom whose hyperfine coupling is being calculated and the subscripts indicate the bond under consideration. In principle, such a nonlocal expression could be used with experimental hyperfine values to derive self-consistent values for $\varrho^\pi(C2)$, $\varrho^\pi(C3)$, and $\varrho^\pi(N1)$. However, the constants $Q_{NC}{}^C$ and $Q_{CN}{}^C$ are not well known,[44] and thus it is not possible to make a reliable calculation of $\varrho^\pi(C2)$ knowing only $A_\perp(^{13}C2)$. The same problem arises for N1.

Appendix II

Determination of Trp Indole Spin Densities. The theory for EPR of the exchange-coupled ES complex[23] shows that those molecules that contribute to the peak in the EPR envelope ($g = 2.01$) are oriented such that the magnetic field, $\mathbf{B}_0$, lies along the heme normal (Fe=O bond). The crystal structure[10] then shows that when this subset of molecules is at resonance, the field lies roughly in the indole plane in an orientation sketched in Figure 10. Thus, we can take a proton hyperfine coupling measured at $g = 2.01$ as being equivalent to a single-crystal value corresponding to this field orientation. This model is supported by field-dependent ENDOR measurement. The field orientation assigned to a spectrum at $g = 2.01$ corresponds closely to the maximum value of $A(H1)$ (see below), and thus other orientations should show smaller couplings. To test this assumption, we have examined the $^1H1$ and $^2H1$ resonances,

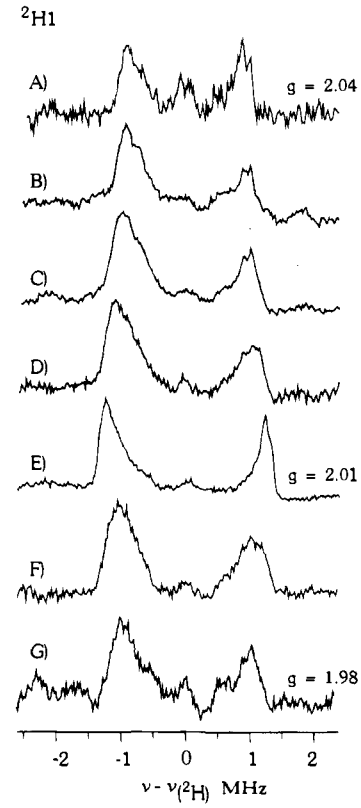

Figure 11. Field dependence of ^2H Q-band Mims pulsed ENDOR. Conditions: magnetic field (A) 12 150, (B) 12 250, (C) 12 300, (D) 12 350, (E) 12 400, (F) 12 450, (G) 12 525; microwave frequency, 34.75 GHz; $\pi/2$ pulse width (A, G) 60 ns, (B–F) 100 ns; $\tau_{rf} = 70\ \mu s$; $\tau_{12} =$ (A) 340 ns, (B–F) 200 ns, (G) 240 ns; repetition rate (A) 30 ms, (B–G) 25 ms; number of scans (A) 20, (B–F) 5, (G) 1.

seen, respectively, in the ENDOR spectra of ES(D_8,H) and ES(H_8,D) (Figure 4C,D), at other fields, including g values both above and below $g = 2.01$ (Figure 11). As illustrated by the $^2H1$ spectra in Figure 11, these signals shift and broaden to lower hyperfine couplings at g values that sample other orientations, thus confirming the assignment.

From the $g = 2.01$ spectra presented above (Figures 4 and 5), for the proton attached to N1 at this orientation, $A(^1H1) = 16$ MHz; for the C2 proton $A(^1H2) = 15$ MHz. To analyze these results, we need explicit expressions for the tensor contributions to eq 6. $\mathbf{A}^{C2}$ and $\mathbf{A}^{N1}$ are well established for an α-proton attached to a C in a π-radical ($\mathbf{A}^{C2}$) and for an α-proton attached to a N in a π-radical ($\mathbf{A}^{N1}$):[45]

$$\mathbf{A}^{C2} = [A_1{}^{C2}, A_2{}^{C2}, A_3{}^{C2}] = [-29, -91, -61] \quad \text{(A3a)}$$

$$\mathbf{A}^{N1} = [A_1{}^{N1}, A_2{}^{N1}, A_3{}^{N1}] = [-26, -116, -75] \quad \text{(A3b)}$$

The principal axes of these tensors are shown in Figure 10 (solid arrows). The components $A_3{}^{C2}$ and $A_3{}^{N1}$ are oriented along the normal to the Trp plane, which is closely perpendicular to the heme normal; the components $A_1{}^{C2}$ and $A_1{}^{N1}$ are along the CH bond and NH bond, respectively; $A_2{}^{C2}$ and $A_2{}^{N1}$ are in the plane of the tryptophan and perpendicular to $A_1{}^{C2}$ and $A_1{}^{N1}$.

The contributions due to through-space interactions from neighboring atoms may be described roughly with the point dipole approximation,[40] in which case the $\mathbf{T}^i{}_j$ are axial, traceless tensors with the unique (maximum) component ($T_\parallel$) along the vector between atom j and proton i. The principal components

(45) Gordy, W. Theory and Applications of Electron Spin Resonance. *Techniques of Chemistry XV*; John Wiley & Sons: New York, 1980.

Table 2. Dipolar Hyperfine Matrices (MHz) (Eq 6) and Field Direction Cosines[a]

$$\mathbf{T}^{H2}{}_{N1} = \begin{vmatrix} 9.1 & 10.4 & 0 \\ 10.4 & -2.1 & 0 \\ 0 & 0 & -6.9 \end{vmatrix} \quad \mathbf{T}^{H2}{}_{C3} = \begin{vmatrix} 7.4 & -9.1 & 0 \\ -9.1 & -1.7 & 0 \\ 0 & 0 & -5.6 \end{vmatrix} \quad l(H2)^b = \begin{pmatrix} 0.839 \\ 0.495 \\ -0.224 \end{pmatrix}$$

$$\mathbf{T}^{H1}{}_{C2} = \begin{vmatrix} 7.9 & -10.3 & 0 \\ -10.3 & -1.8 & 0 \\ 0 & 0 & -6.1 \end{vmatrix} \quad \mathbf{T}^{H1}{}_{C3} = \begin{vmatrix} 4.3 & -1.7 & 0 \\ -1.7 & -2.1 & 0 \\ 0 & 0 & -2.2 \end{vmatrix} \quad l(H1)^b = \begin{pmatrix} -0.143 \\ 0.975 \\ -0.17 \end{pmatrix}$$

[a] Dipolar tensors were calculated using the method described by McConnell and Strathdee[41] and expressed in the appropriate local proton frame (Figure 10) as described in the text. [b] Direction cosines with respect to local coordinate frame of magnetic field along heme normal. See text and Figure 10.

for unit spin are $T_{\|}{}^{i}{}_{j} = 2\mu_e\mu_n/(r^{i}_{j})^3$, where r^{i}_{j} is the distance from the proton i to atom j, and $T_{\perp}{}^{i}{}_{j} = -T_{\|}{}^{i}{}_{j}/2$. The C2−H1 and C3−H2 distances are sufficiently small (~2.2 Å), and some spin densities are sufficiently high that we performed the more elaborate calculation in which we consider the spin density on a C or N to be distributed over a Slater $2p_\pi$ orbital and calculate the dipolar tensor according to McConnell and Strathdee.[41] In Figure 10, the r^{i}_{j} vectors for this calculation lie in the plane of the Trp and are displayed as dashed arrows originating at the protons on C2 and N1, respectively. For H2, the point dipole unit spin values are $T_{\|}{}^{H2}{}_{N1}$ = 17.9 MHz and $T_{\|}{}^{H2}{}_{C3}$ = 16.6 MHz, and for H1, $T_{\|}{}^{H1}{}_{C2}$= 19.0 MHz and $T_{\|}{}^{H1}{}_{C3}$ = 5.3 MHz. For comparison, "$T_{\|}{}^{H2}{}_{C3}$" = 13.0 MHz following McConnell and Strathdee. In the end, the two calculations gave indistinguishable results.

For H2, the three interactions in eq 6a are summed by transforming $\mathbf{T}^{H2}{}_{N1}$ and $\mathbf{T}^{H2}{}_{C3}$ into the coordinate frame defined by the H2 local hyperfine tensor, $\mathbf{A}^{H2}$, using the standard rotation matrix;[46] the angle between the $A_1{}^{H2}$ direction and $r^{H2}{}_{N1}$ is θ = 30.82°, and the angle between the $A_1{}^{H2}$ and $r^{H2}{}_{C3}$ for C3 is ψ = −31.69°. The equivalent was done for H1, eq 6b, by transforming $\mathbf{T}^{H1}{}_{C2}$ and $\mathbf{T}^{H1}{}_{C3}$ into the H1 frame, where the angle between $A_1{}^{H1}$ and $r^{H1}{}_{C2}$ is −32.47° and the angle between $A_1{}^{H1}$ and $r^{H1}{}_{C3}$ is −13.63°. The nonlocal dipolar hyperfine tensors of eq 6 as calculated according to McConnell and Strathdee and rotated into the local frame are listed in Table 2.[41]

The transition frequencies for nucleus i at field orientation l, $\nu_{\pm}l(i)$, and thus the hyperfine coupling at this orientation, $A^{l}(i)$, can be calculated to adequate precision by ignoring **g** anisotropy in the standard expression[47]

$$\nu_{\pm}l(i) = \{l\cdot[(\pm 1/2)\mathbf{A}(i)_{tot} - \nu_H\mathbf{I}]^2\cdot l\}^{1/2} \qquad \text{(A4a)}$$

$$A^{l}(i) = \nu_{+}l(i) - \nu_{-}l(i) \qquad \text{(A4b)}$$

In the equation, l is the unit vector along the magnetic field $\mathbf{B}_0$ (see Figure 10), $\mathbf{I}$ is the identity matrix, and ν_H is the proton Larmor frequency. In fact, at the fields employed in Q-band ENDOR direct comparison shows that the high-field approximation is valid, in which case

$$A^{l}(i) = l\cdot\mathbf{A}(i)_{tot}\cdot l \qquad \text{(A5)}$$

For the measurements at g = 2.01, the field ($\mathbf{B}_0$) lies along the heme normal and thus to a first approximation lies in the plane of the indole ring at an angle Ω from the A_1 axis of the local H1 and H2 hyperfine coordinate frames (Figure 10) where Ω ≈ 98° for H1 and Ω ≈ 32° for H2. The actual direction cosines for the field within the H2 coordinate frame are l(H2) = [0.839, 0.495, −0.224]; those in the H1 coordinate frame are l(H1) = [−0.143, 0.975, −0.17]. The g = 2.01 hyperfine couplings measured in ENDOR experiments are then equated to eq A4b.

If we take ϱ^{π}(C3) = 0.41 as determined above, then the values of A(H1) and A(H2) measured at g = 2.01 allow us to calculate ϱ^{π}(C2) and ϱ^{π}(N1), through eqs 6 and A4. As the resulting relations between the couplings and the spin densities are nonlinear in the latter, it proved simplest to determine the spin densities iteratively. First, a crude estimate of the spin density on C2 was obtained from $\mathbf{A}(H2)_{tot}$ (eq 6a) by setting ϱ^{π}(N1) = ϱ^{π}(C3) = 0. This value, ϱ^{π}(C2) = 0.33, was used with ϱ^{π}(C3) in eq 6b, allowing ϱ^{π}(N1) to be calculated from eqs 6 and A4. This was done graphically by plotting the calculated values of A(H1) (eq A4b) and comparing with the measured value of A(H1). The resulting value of ϱ^{π}(N1) was then used in graphically obtaining ϱ^{π}(C2). This process was repeated until self-consistency was obtained. We find that the nonlocal terms have only a minor effect, even from centers with high spin density. Thus, the final results are ϱ^{π}(C2) = 0.35 and ϱ^{π}(N1) = 0.14, whereas the corresponding values when omitting nonlocal terms are 0.33 and 0.14, respectively. Among other things this justifies neglect of nonlocal contributions from atoms with smaller spin densities.

The direction cosines for the field in the H6 frame are l(H6) = [−0.572, 0.812, 0.089]. We calculated ϱ^{π}(C6) from $A(^1H6)$ = 5 MHz by ignoring non-local contribution to A(H6) and assigning a negative value based on the Hückel−McLachlan calculation.

The uncertainties in the experimental spin densities are of course dependent upon the uncertainties in the unit spin parameters for the α- and β-protons.[38,45] However, because the data are from one orientation, and are not redundant as would be the case for a full tensor determination, for the α-protons H1 and H2 they are also, and likely to a greater extent, dependent on the precise assumption of the direction of the zero field splitting axis. Although the Fe=O bond has been found to be near the heme normal,[18] we have examined this by allowing the Fe=O direction to explore a cone angle of ~3° about the heme normal. This produces uncertainties of less than ±6% in the reported spin densities for N1 and C2.

JA951010G

(46) Mathews, J.; Walker, R. L. *Mathematical Methods of Physics*; W. A. Benjamin, Inc.: New York, 1965.

(47) Hoffman, B. M.; Gurbiel, R. J.; Werst, M. M.; Sivaraja, M. In *Advanced EPR. Applications in Biology and Biochemistry*; Hoff, A. J., Ed.; Elsevier: Amsterdam, 1989; pp 541−591.